

# Efficient and accurate determination of mode I type 3-D surface crack by measuring strain around the crack on the idea of the body force method

DAI-HENG CHEN<sup>1</sup>, NAO-AKI NODA<sup>2</sup>, KAZUHIRO ODA<sup>2\*</sup> and SHOJI HARADA<sup>2</sup>

<sup>1</sup>*Department of Mechanical System Engineering, Kyushu Institute of Technology, 680-4 Kawazu, Iizuka 820, Japan*

<sup>2</sup>*Department of Mechanical Engineering, Kyushu Institute of Technology, 1-1 Sensui-cho, Tobata, Kitakyushu 804, Japan*

Received 18 September 1994; accepted in revised form 10 April 1995

**Abstract.** In this study, the location and the size of a three-dimensional semi-elliptical surface crack in a semi-infinite body are detected from data of strains measured around a region of the crack. Also the loading stress at infinity is treated as an unknown parameter. The crack location, size and the loading stress are determined through the condition which minimizes the square sum of residuals between measured strain distributions and computed ones for an assumed crack. The body force method is used to calculate the strain field around the crack. In order to obtain the solution with short CPU time, the crack is represented by a set of force doublets, and the database of the magnitudes of force doublets for various aspect ratios of the crack is utilized. The method of gradient search is employed to find out an optimal set of parameters. The fact that the strain field around the surface crack is mainly dominated by the crack area is utilized in detecting the crack. Several inversion schemes are examined to obtain accurate results. Numerical simulations are carried out and the results show that crack location, shape and loading stress are determined efficiently with good accuracy.

## 1. Introduction

Detecting and sizing surface cracks are the prerequisites of an evaluation of the remaining strength of structures based on fracture mechanics. Recently, crack detection has been regarded as one of the inverse problems. Quantitative measurement of cracks and defects based on the application of inverse analysis has been made by a lot of researchers using D.C. or A.C. electric potential method [1–5], ultrasonic method [6,7], elastodynamic method [8] and strain measurement [9], etc. [10,11]. Analysis of inverse problems has been generally carried out through the iteration of direct analyses developed so far. In the inverse problem of 3-D crack identification, however, a large number of iterations of the direct analysis must be performed to determine a lot of unknown parameters, such as crack location and size, etc. Then large scale analysis has to be performed using supercomputers. Therefore it is difficult to apply those methods to the practical measurement of the crack.

In this study, the location and the size of the semi-elliptical surface crack are detected from data of strains measured around a region involving the crack. In order to carry out high-speed computation on a standard workstation, an efficient method of inverse analysis is proposed on the basic concept of body force method. The body force method [12,13] is known as one of the most useful numerical methods for the stress analysis of various crack problems. On the idea of the body force method, strain field due to a crack can be represented by embedded body force doublets in the structure without a crack. Thus, the search for the location and the

---

\* Current address: Department of Mechanical and Electrical Engineering, Tokuyama College of Technology, 3538 Takajo, Kume, Tokuyama 745, Japan.

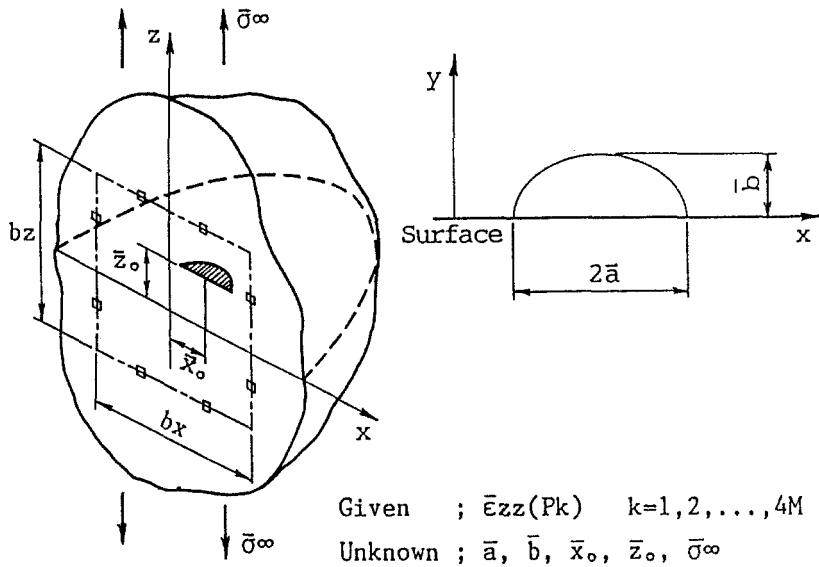


Fig. 1. Problem of 3-D surface crack identification.

shape of the crack is reduced to determining the location and the magnitude of these force doublets so as to produce the most similar strain field around the crack. By extending this concept, the efficient analysis scheme is developed. Moreover, in order to obtain the solution accurately, several inversion schemes are examined and numerical experiments are carried out to investigate the usefulness of the proposed method.

### 2. Efficient determination of crack using the body force method

In this section, by solving the inverse problem of a three-dimensional surface crack, the method of inverse analysis based on the body force method will be explained. Consider a semi-infinite solid containing a semi-elliptical surface crack under uniform stress  $\bar{\sigma}^\infty$  at infinity as shown in Fig. 1. Here, actual crack center locations  $\bar{x}_0, \bar{z}_0$ , an actual surface crack length  $2\bar{a}$  and an actual crack depth  $\bar{b}$  are unknown. In addition, the loading stress  $\bar{\sigma}^\infty$  is also treated as an unknown parameter because the applied stress in structures usually changes every moment and cannot be known in advance. As the information to identify the crack, strains  $\bar{\epsilon}_{zz}(P_k)$  measured at points  $P_k (k = 1, \dots, 4M)$  are used. Then, the problem is to determine five unknown parameters  $x_0, z_0, a, b$  and  $\sigma^\infty$  on the basis of the data of strains measured at the points  $P_k$ .

The inverse problem is analyzed by iteration of a direct analysis. When the unknown parameters  $x_0, z_0, a, b$  and  $\sigma^\infty$  are assumed, the corresponding strains at the points  $P_k$  can be calculated through straightforward computation. Then, the strains  $\epsilon_{zz}(P_k)$  corresponding to the assumed parameters are compared with the measured strains  $\bar{\epsilon}_{zz}(P_k)$  through the following function

$$R = \sum_{k=1}^{4M} \{ \epsilon_{zz}(P_k) - \bar{\epsilon}_{zz}(P_k) \}^2. \tag{1}$$

Here,  $R$  is called the objective function. If assumed parameters  $x_0, z_0, a, b$  and  $\sigma^\infty$  are close to the actual ones, the objective function  $R$  becomes small because the computed strains

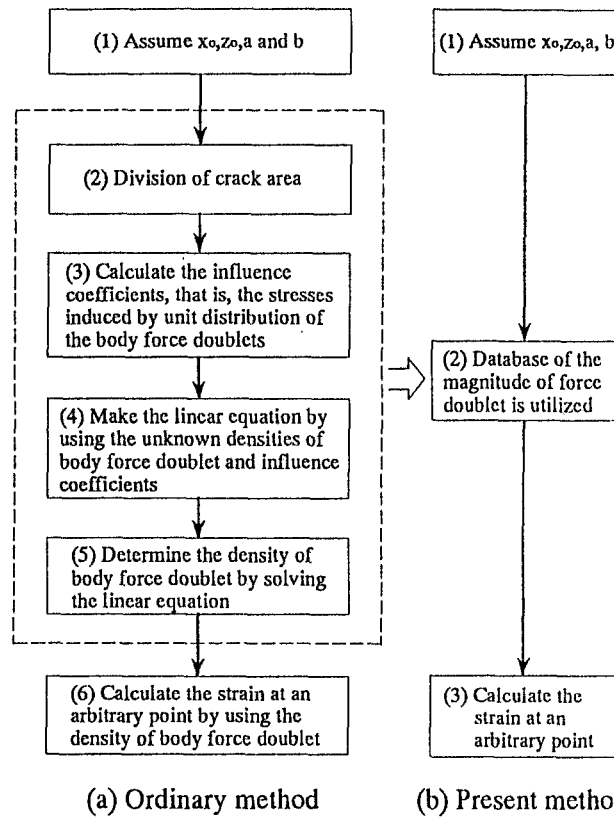


Fig. 2. Flow chart of the body force method to calculate strains due to a crack.

$\varepsilon_{zz}(P_k)$  are close to the measured strains  $\bar{\varepsilon}_{zz}(P_k)$ . Therefore the inverse analysis is reduced to searching for the optimal set of parameters  $x_0, z_0, a, b$  and  $\sigma^\infty$  which minimizes the objective function  $R$ .

In principle, the optimal set of parameters may be obtained through trial and error of the direct analysis. However, it is actually impossible to obtain the optimal set of parameters only through trial and error because the number of all possible combinations of the five unknown parameters is so enormous. Then it is essential to find how to reduce the calculation time necessary to find out the solution. In this study, in order to shorten the calculation time, the following method of the inverse analysis is proposed.

2.1. EFFICIENT CALCULATION OF STRAINS AROUND THE CRACK

It is important to shorten the CPU time necessary for one time calculation of the direct analysis because a large number of iterations must be made. In the calculation of the strain for the assumed parameters, the body force method is employed. In this method, a crack is replaced by distribution of body force doublets in the semi-infinite solid without the crack [12,13]. The strain at the measured point  $P_k$  is calculated from the density of body force doublet, as shown in the following equation

$$\varepsilon_{ij}(P_k) = \varepsilon_{ij}(P_k, \infty)\sigma^\infty + \int \int_S \varepsilon_{ij}(P_k, Q)T(Q) dQ, \tag{2}$$

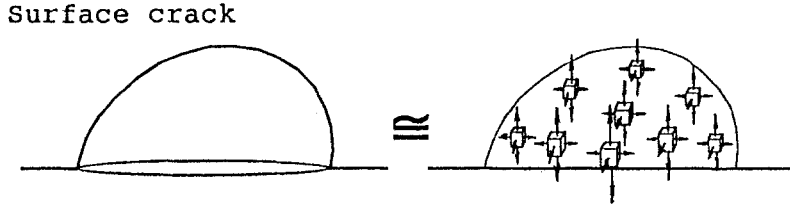


Fig. 3. Approximation method to calculate the strain field around the crack.

where  $\varepsilon_{ij}(P_k, \infty)$  is the strain at a point  $P_k$  due to the uniform stress  $\sigma^\infty = 1$  at infinity in the semi-infinite solid without the crack,  $\varepsilon_{ij}(P_k, Q)$  is the strain at a point  $P_k$  due to the set of point force doublets with unit magnitude acting at a point  $Q$ , and  $S$  is the prospective domain of the crack. The flow chart of analysis based on (2) is shown in Fig. 2(a), where most of the running time is consumed for determining the density of body force doublet (illustrated step (2) ~ (5) in Fig. 2(a)). To simplify the calculation of the strains, in this study, the following method will be proposed.

As shown in Fig. 3, the crack is assumed to be approximated by discrete force doublets applied at nine points instead of continuous distribution of force doublets. These discrete force doublets are named ‘giant force doublets’. From Fig. 3, the strain at the point  $P_k$  is expressed by

$$\varepsilon_{ij}(P_k) = \varepsilon_{ij}(P_k, \infty)\sigma^\infty + \sum_{n=1}^9 \varepsilon_{ij}(P_k, Q_n)T_n, \quad (3)$$

where  $\varepsilon_{ij}(P_k, Q_n)$  is strain  $\varepsilon_{ij}$  at a point  $P_k$  in the semi-infinite solid due to the giant force doublet with unit magnitude acting at a point  $Q_n$ . In (3), the magnitude of the giant force doublet  $T_n$  is determined by integrating the density of the body force doublet,  $T(Q)$ , in each subdomain shown in Fig. 4. In this study, the magnitude of the giant force doublet  $T_n$  is calculated beforehand and is stored in a computer file as a database. The magnitude of force doublet varies smoothly depending on the aspect ratio  $b/a$  and can be expressed as a simple function of  $b/a$ .

$$T_n = \frac{4(1 - \nu)^2 ab^2 \sigma^\infty}{(1 - 2\nu)} f_n(b/a), \quad (n = 1, \dots, 9), \quad (4)$$

$$\begin{aligned} f_1(b/a) &= 0.22019 - 0.012487(b/a) + 0.02983(b/a)^2 - 0.001684(b/a)^3, \\ f_2(b/a) &= 0.18256 - 0.10171(b/a) + 0.02441(b/a)^2 - 0.001484(b/a)^3, \\ f_3(b/a) &= 0.17746 - 0.10037(b/a) + 0.02487(b/a)^2 - 0.001631(b/a)^3, \\ f_4(b/a) &= 0.10008 - 0.05068(b/a) + 0.00992(b/a)^2 - 0.000102(b/a)^3, \\ f_5(b/a) &= 0.09851 - 0.05223(b/a) + 0.01156(b/a)^2 - 0.000479(b/a)^3, \\ f_6(b/a) &= 0.09932 - 0.05554(b/a) + 0.01411(b/a)^2 - 0.001060(b/a)^3. \end{aligned} \quad (5)$$

The subscripts in (5) correspond to the number of subdomain shown in Fig. 4. Since the giant force doublets are symmetrically distributed with respect to  $\eta$ -axis, only the six equations are needed as the database. Each of the coefficient in (5) are determined by the least square

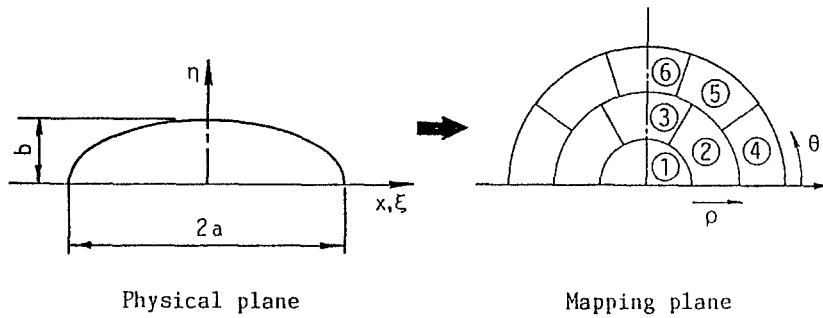


Fig. 4. Mapping and dividing of crack area.

regression method. Usually, the strain distribution far from the crack can be available as a piece of information to identify the crack. Since the error of strain due to the giant force doublets decreases rapidly with increasing the distance from the crack, the proposed method is good enough to represent the strain field except near the crack. Namely, as shown in Fig. 2(b), with the aid of the database, the computation of strain can be made easily and the running time can be reduced.

2.2. EFFICIENT METHOD OF GRADIENT SEARCH

To find out rapidly the optimal set of the parameters which minimize the objective function  $R$ , the method of gradient search is applied. In this method, the gradient vector of the objective function  $R$  at the assumed set of unknowns is calculated and the assumed point is modified iteratively in the most improved direction of  $R$  [9]. However, if this method is applied, it is found that there are two major difficulties in the process of searching the optimum condition.

(A) To determine the searching direction it is necessary to calculate numerically the derivative of the objective function with respect to all of the parameters to be searched.

(B) Since only the local information for assumed parameters is used, the results obtained by the gradient search tend to be drawn to a local minimum instead of the true minimum.

In this study, to avoid such difficulties the following scheme is proposed [9].

2.2.1. Reduction of the number of parameters to be searched

In order to determine the searching direction with short CPU time, it is preferable to decrease the number of parameters to be searched. As shown in (3) and (4), the strain due to the crack can be expressed as a linear function of  $\sigma^\infty$ . On the basis of this fact, the value of  $\sigma^\infty$  can be directly obtained by the following equation

$$\partial R / \partial \sigma^\infty = 0. \tag{6}$$

Therefore, in this study, the method of gradient search is applied only for the four parameters  $x_0, z_0, a, b$ .

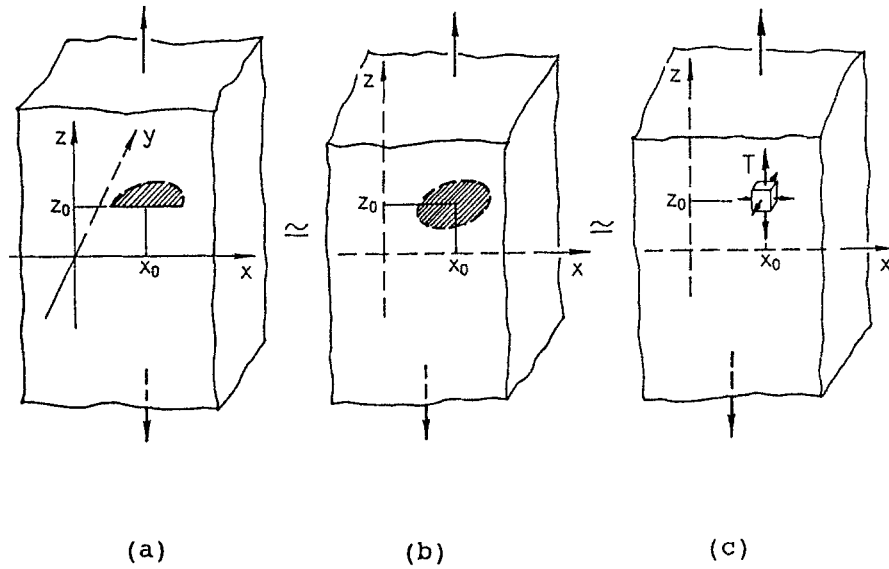


Fig. 5. Approximation method to select the starting point.

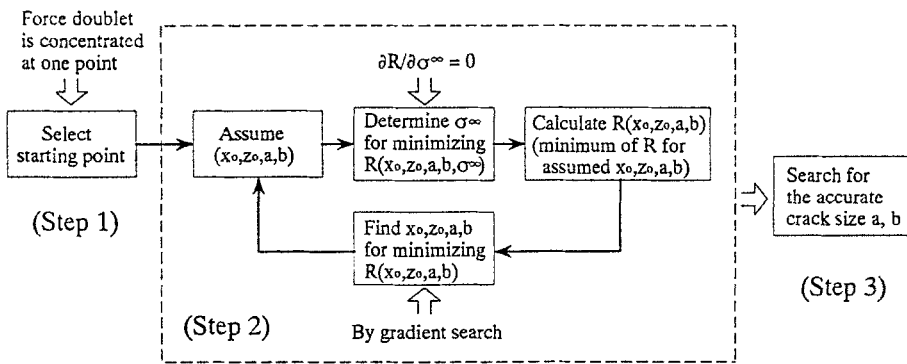


Fig. 6. Basic procedure of proposed inverse analysis.

2.2.2. *Efficient determination of the starting point of gradient search*

To avoid the difficulty due to the local minimum, the most promising starting point for the gradient search should be selected. This can be determined by using the concept of the body force method.

As shown in Fig. 5, the strain field due to the surface crack is simply approximated by the single embedded giant force doublet with magnitude  $T$  in an infinite solid. The most suitable initial values of unknown parameters,  $x_{0s}$ ,  $z_{0s}$  and  $T_s$ , are determined by the condition which minimizes  $R$ . For certain points suitably chosen in the searching region, the value of  $R$  can be calculated. Since the strain field in Fig. 5(c) is expressed as a linear function of  $T$  as well as  $\sigma^\infty$ , the values of  $T$  and  $\sigma^\infty$  are directly obtained from the condition

$$\partial R / \partial T = 0, \quad \partial R / \partial \sigma^\infty = 0. \tag{7}$$

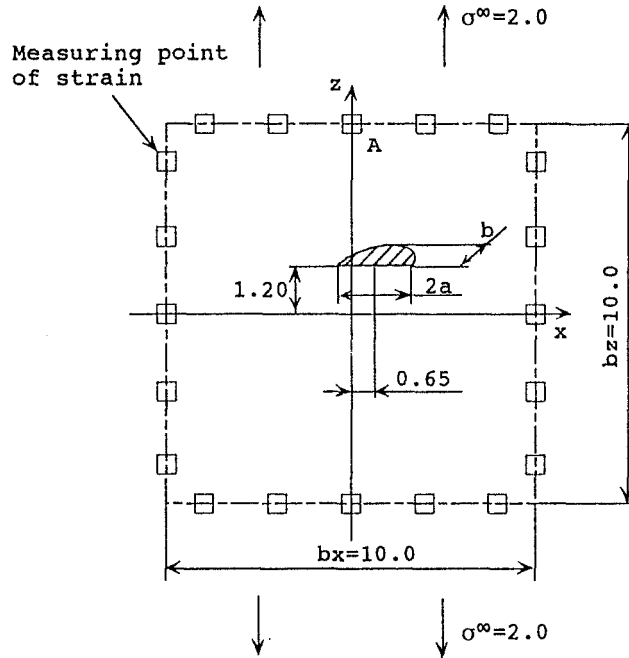


Fig. 7. Problem examined in Section 3.

Through the comparison of  $R$ -values, the point with the smallest value of  $R$  is selected as the starting point  $x_{0s}, z_{0s}$ . The initial value of the crack size is estimated by the following expression on the assumption of the circular crack ( $a_s = b_s$ , see Appendix)

$$a_s = \sqrt[3]{\frac{3(1-2\nu)T_s}{16(1-\nu)^2\sigma^\infty}} \quad (8)$$

The gradient search started from these values  $x_{0s}, z_{0s}, a_s, b_s$  can reach the true minimum of  $R$  without the difficulty of a local minimum.

### 3. Accurate determination of crack size

As shown in Fig. 6, the problem is solved in the process of two main steps.

(Step 1) Select the starting point of the gradient search.

(Step 2) Search for the solution by using the method of gradient search from the selected starting point.

When the method of gradient search is applied for the four unknowns  $x_0, z_0, a, b$ , the crack center location  $x_0, z_0$  is estimated earlier and the crack size  $a, b$  is obtained later. However, the crack size  $a, b$  cannot be determined very accurately compared with the crack location  $x_0, z_0$ . Thus, it is necessary to introduce the third procedure (Step 3) to determine the accurate crack size (see Fig. 6).

In this study, several inversion schemes are proposed and examined to estimate the crack size  $a, b$  accurately. First, since the crack location is estimated accurately at (Step 2), the crack location is fixed and the gradient search is carried out only for two parameters  $a, b$ . This scheme is named 'method (a)'. Next, as 'method (b)', the crack area  $S$  and aspect ratio  $b/a$  are chosen

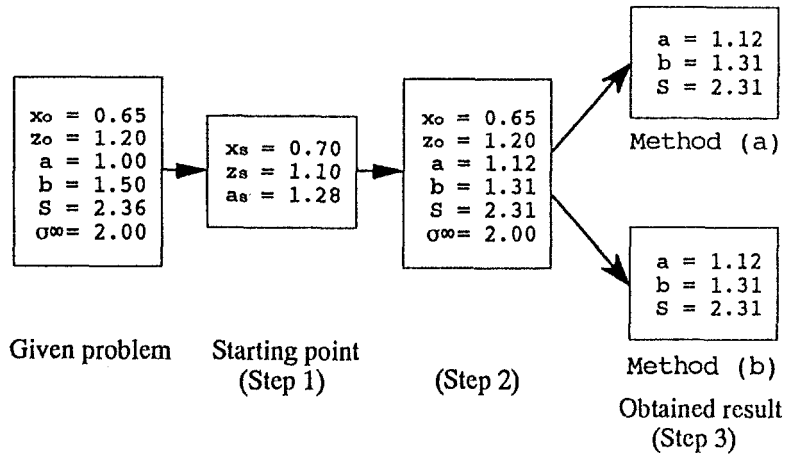


Fig. 8. Results obtained by method (a) and method (b).

as searching parameters instead of the crack size  $a, b$ , and the gradient search is performed after (Step 2). To compare both methods, the problem shown in Fig. 7 is analyzed. The results in Fig. 8 show that the crack size cannot be determined with good accuracy by either method (a) or (b). However, it should be noted that the crack area  $S = \pi ab/2$  is estimated accurately within 2 percent error. This suggests that the strain field around the crack is mainly dominated by the crack area  $S$  [14] and therefore other parameters such as  $b/a$  cannot be determined accurately using the method of gradient search.

In the following section, the effect of crack parameters on the strain field around the crack will be discussed in more detail.

### 3.1. EFFECT OF THE CRACK SIZE ON THE STRAIN FIELD

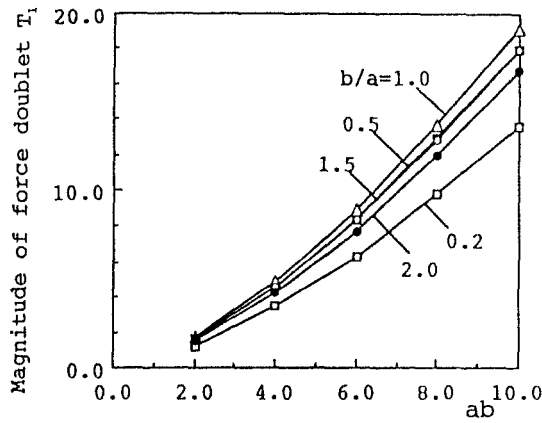
In the body force method, the strain due to a crack is calculated from the influence coefficient  $\varepsilon_{ij}(P_k, Q_n)$  and the magnitude of force doublet  $T_n$  as shown in (3). Based on this idea the strain is found to be closely related to  $T_n$ . The magnitude  $T_n$  defined by (4) becomes

$$T_n = \frac{4(1-\nu)^2}{(1-2\nu)} \left(\frac{2}{\pi}S\right)^{3/2} (b/a)^{1/2} f_n(b/a). \tag{9}$$

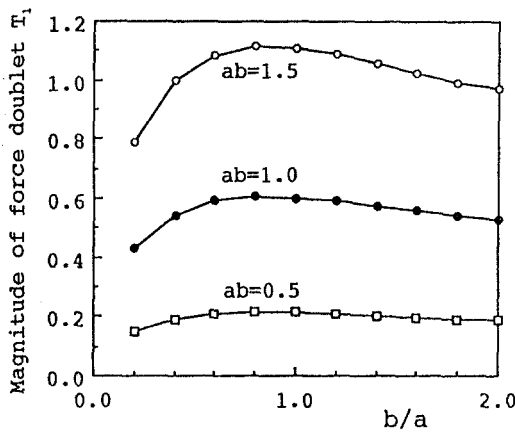
As shown in (9),  $T_n$  is proportional to  $S^{3/2}$ . As an example, the  $T_1 - ab$  relation and  $T_1 - b/a$  relation are shown in Fig. 9. Here, the parameter  $ab$  is double the size of the crack area. As shown in Fig. 9,  $T_1$  increases in proportion to  $(ab)^{3/2}$  when  $b/a = \text{constant}$ . On the other hand, when  $ab = \text{constant}$  the variation of  $T_1$  is about 10 percent in the range  $0.5 \leq b/a \leq 2.0$ . A similar discussion can be applied to  $T_2 \sim T_6$ . Since the magnitude of force doublet  $T_n$  is mainly dominated by the crack area  $S$ , the strain field is also controlled by  $S$  [14].

Next, the variation of strain  $\varepsilon_{zz}$  at the point  $A$  shown in Fig. 7 is examined with varying crack size  $a, b$ . First, the  $\varepsilon_{zz} - ab$  relation is shown in Fig. 10(a) when  $b/a$  is constant. Here, the strain  $\varepsilon_{zz}$  is normalized by the strain at infinity  $\varepsilon_{zz}^\infty$ . Next, Fig. 10(b) shows the  $\varepsilon_{zz} - b/a$  relation under the constant value of  $ab$ . From Fig. 10, it is found that the variation of the strain under  $ab = \text{constant}$  is small in the range  $0.5 \leq b/a \leq 2.0$ , that is, the variation of the crack aspect ratio has only small effect on the strain around the crack. In other words, the strain distribution around the surface crack is mainly dominated by the crack area.





(a)



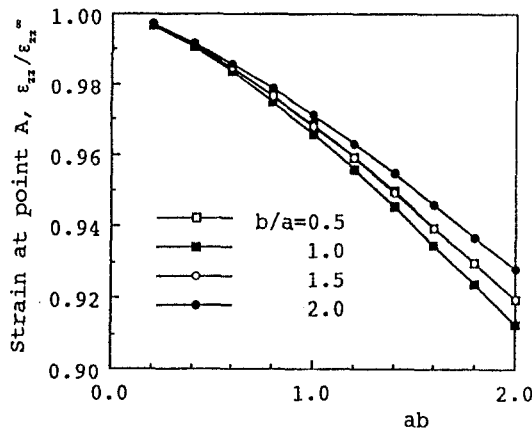
(b)

Fig. 9. (a) Effect of  $ab$  on  $T_1$  when  $b/a = \text{constant}$  and  $\sigma^\infty = 1$ , and (b) Effect of  $b/a$  on  $T_1$  when  $ab = \text{constant}$  and  $\sigma^\infty = 1$ .

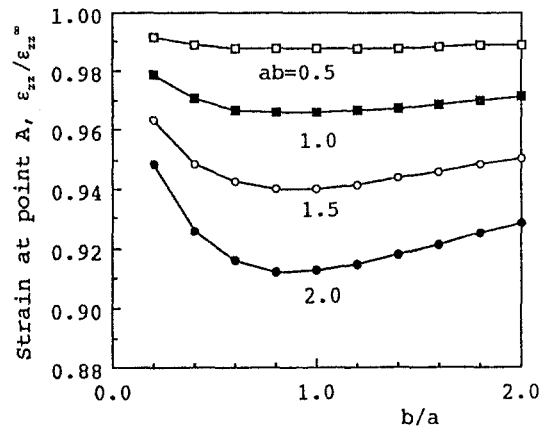
Furthermore, the relations between the objective function  $R$  and the parameters  $ab$  or  $b/a$  are also investigated. Figure 11 shows the variation of  $R$  under the condition that  $b/a = \text{constant}$  or  $ab = \text{constant}$ . In the case of  $b/a = \text{constant}$ , the objective function  $R$  varies significantly with  $ab$  having a true minimum at  $ab = 1.5$ . On the other hand, in the case of  $ab = \text{constant}$ , the values of  $R$  are almost zero and the variation of  $R$  is small. From Fig. 11(a) it is seen that if the parameter  $ab$  is close to the true value, the  $R$ -value is close to zero even when  $b/a$  is far different from the true value. The detailed variation of  $R$  is plotted in Fig. 11(b), where the ordinate represents  $\log R$ . Figure 11(b) shows that when  $ab = \text{constant}$  the function  $R$  is almost less than  $10^{-5}$  having a local minimum at  $b/a \approx 0.5$ . Figure 11(b) shows us the reason why the determination of crack size is difficult. The reason is that the  $R$ -value has some local minima causing difficulties in searching for the true minimum.

The discussion mentioned above leads to the conclusions:

- (1) The strain distribution around the surface crack is mainly dominated by the crack area almost irrespective of crack aspect ratio.



(a)



(b)

Fig. 10. (a) Effect of  $ab$  on strain at point A when  $b/a = \text{constant}$ , and (b) Effect of  $b/a$  on strain at point A when  $ab = \text{constant}$ .

- (2) When the crack area is close to the true value,  $R$ -value is almost zero and the variation of  $R$  has some local minima. This is the reason why the crack aspect ratio is difficult to determine compared with the crack area by only using the methods (a) and (b).
- (3) To estimate the crack size accurately, it is necessary to introduce the new method to overcome the difficulty due to local minimum.

### 3.2. PROCEDURE OF SEARCHING FOR ACCURATE CRACK SIZE

In the ordinary method of gradient search such as methods (a) and (b), since the modification of crack aspect ratio is very small, the obtained results are drawn to a local minimum. If all ranges of  $b/a$  can be examined, the true minimum of  $R$  can be searched because the true minimum of  $R$  is smaller than the local minimum as illustrated in Fig. 11.

In the discussion in Section 3.1, method (c) is proposed as follows using the crack area  $S$  and the crack aspect ratio  $b/a$  as the determining parameters. First, the crack aspect ratio  $b/a$  is assumed within the range  $0 \leq b/a \leq 2.0$  at the intervals of 0.1. Next, under each value of

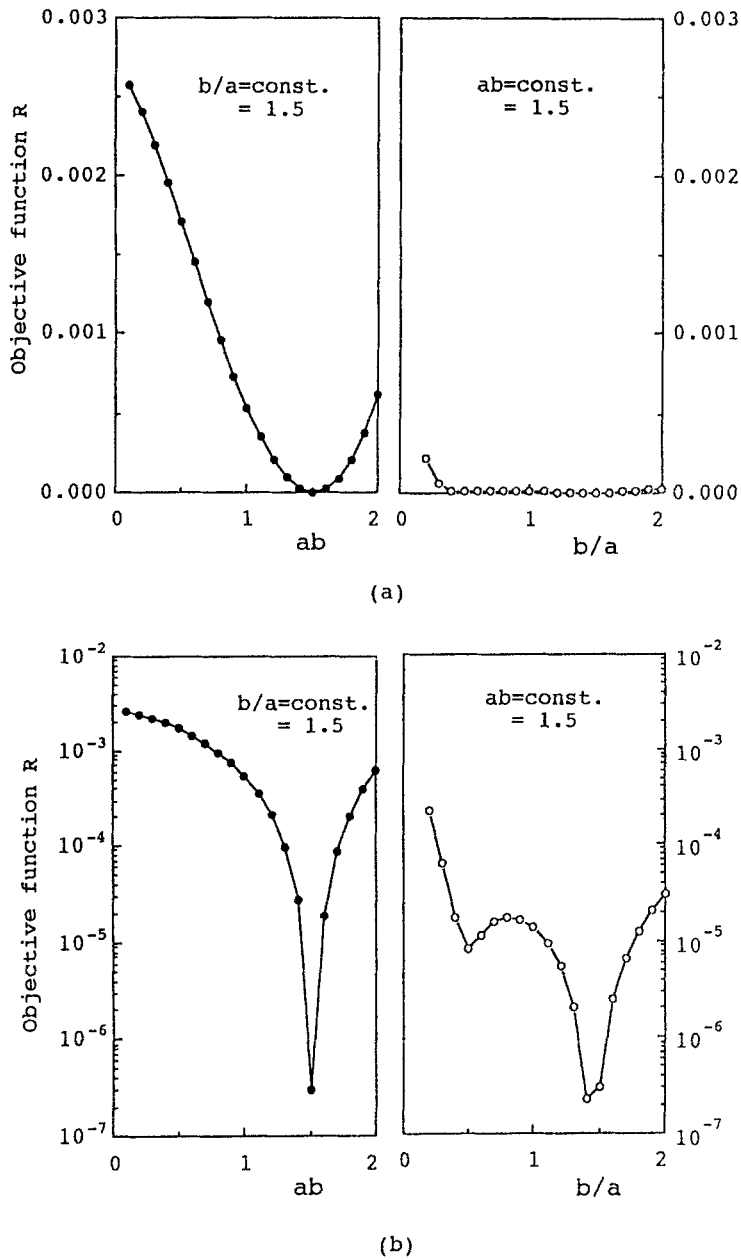


Fig. 11. Relations between objective function  $R$  and parameters  $ab$  or  $b/a$ : (a) ordinate represents  $R$ , and (b) represents  $\log R$ .

assumed  $b/a$ , the most suitable crack area  $S$  can be determined by the condition of minimizing  $R$  using the method of gradient search. At that time, the parameter to be searched is the crack area only. Finally, through the comparison of the obtained  $R$ -values for all the assumed  $b/a$ , the most suitable crack size  $a, b$  can be obtained from the set of  $S$  and  $b/a$ . Figure 12 shows the flow chart of this procedure. In this procedure, first,  $b/a$  is roughly estimated at the interval of 0.1. Second, the aspect ratio is assumed at the intervals of 0.01 near the most suitable value of  $b/a$ , then the same searching procedure is performed again. The result obtained by method

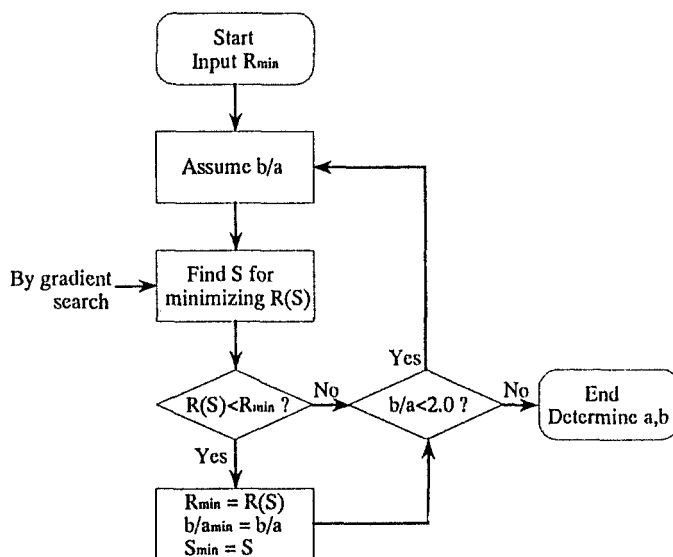


Fig. 12. Flow chart of the search for the accurate crack size [method (c)].

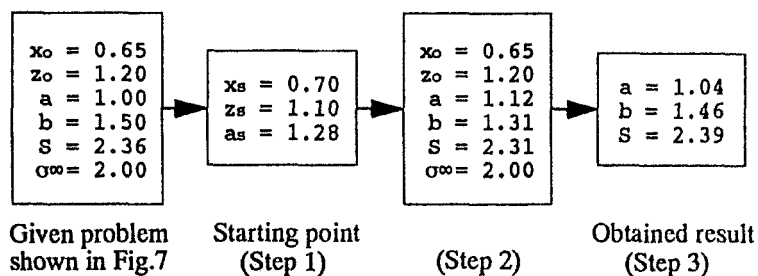


Fig. 13. Result obtained by proposed method [method (c)].

(c) is shown in Fig. 13. Figure 13 shows that the proposed method is found to be useful for searching the crack size accurately.

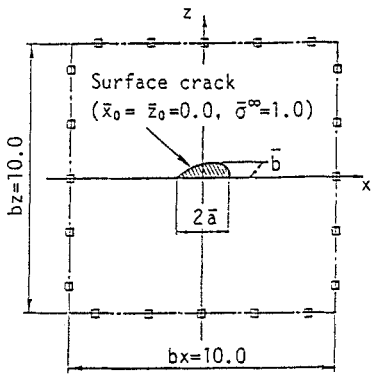
#### 4. Numerical results and discussion

The numerical experiment for determining the crack location, the crack size and the loading stress is carried out to confirm the usefulness of the proposed method. Here, the strains due to the real cracks obtained by the direct analysis are used as ‘measured’ reference data instead of the actually measured data. The data of strains is calculated exactly by the ordinary body force method shown in Fig. 2(a). The analysis is made using the workstation SUN ELC 4/25 FM-8, and the CPU time needed to solve the inverse problem is very short, about one minute.

Table 1 shows the results of the problem for various crack depths  $b$  when the measuring region  $bx = 10, bz = 10$  and the number of points  $M = 5$ . By comparing the given problems with the obtained results, it is found that the five unknowns, the crack location  $x_0, z_0$ , the crack size  $a, b$  and the loading stress  $\sigma^\infty$ , are determined with good accuracy in the range  $b/a \leq 2.0$ .

In general, when the measuring regions  $bx, bz$  become larger or the crack becomes smaller, it becomes difficult to obtain accurately the solution because the strain induced by the crack

Table 1. Results of inverse analysis for various crack depth  $b$

	Given problem		Obtained result				
	$\bar{a}$	$\bar{b}$	$a$	$b$	$x_0$	$z_0$	$\sigma^\infty$
	1.000	0.200	1.019	0.204	0.004	-0.000	1.00
	1.000	0.400	1.020	0.408	-0.000	0.000	1.00
	1.000	0.600	1.017	0.610	0.000	0.000	1.00
	1.000	0.800	1.014	0.811	0.000	0.000	1.00
	1.000	1.000	1.022	1.002	0.000	0.000	1.00
	1.000	1.200	1.023	1.197	0.000	0.000	1.00
	1.000	1.400	1.025	1.394	0.000	0.000	1.00
	1.000	1.600	1.026	1.590	0.000	0.000	1.00
	1.000	1.800	1.026	1.785	0.000	0.000	1.00
	1.000	2.000	1.030	1.957	0.000	0.000	1.00

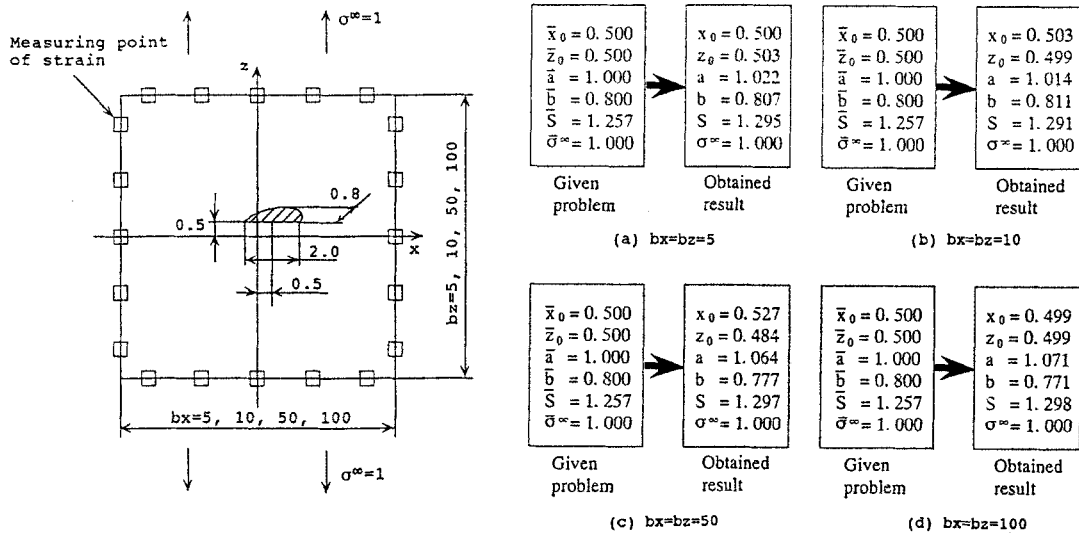


Fig. 14. Results of inverse analysis for various values of  $bx$  and  $bz$  ( $M = 5$ ).

decreases. Figure 14 shows the results of the problem for various values of  $bx$  and  $bz$ . As shown in Fig. 14, it is found that the proposed method is useful in the range  $a/bx \leq 1/100$ .

In this study, since the crack is replaced by the discrete force doublets at nine points, the accuracy of the present result decreases with decreasing the distance between the crack and the measured point  $P_k$ . Figure 15 shows the results of the problem for the variation of the distance  $d$  between the crack location and the measured point. From Fig. 15, it is found that the proposed method is useful when the distance between the crack location and the measured point is larger than the half size of surface crack length  $a$ .

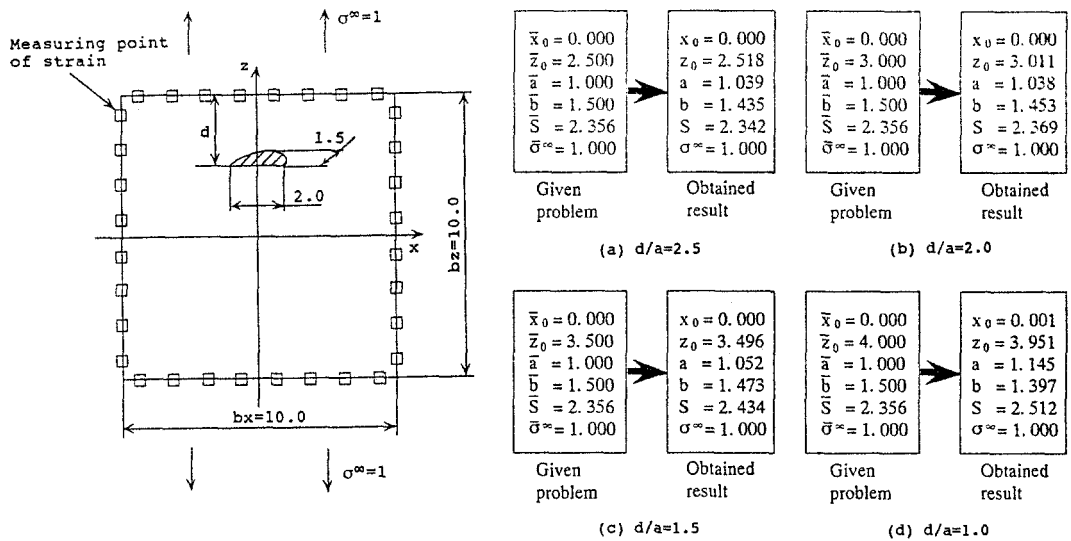


Fig. 15. Results of inverse analysis for various values of distance  $d$  between crack location and measured point ( $b_x = b_z = 10, M = 8$ ).

### 5. Conclusion

In this study, the location and the size of the 3-D surface crack and the loading stress were detected by the data of the strains measured around the region of the crack. The conclusions are summarized as follows:

(1) An efficient inverse scheme was proposed on the basis of the body force method, where the crack was represented by a set of force doublets. In the calculation of strains, the magnitudes of these force doublets were stored as a database for various aspect ratios of the crack. By using the database, the strain around the crack was calculated easily with short CPU time.

(2) To estimate crack size accurately, the effect of unknown parameters on the strain field were investigated. As a result, it was found that the strain field around the surface crack is mainly dominated by the crack area and therefore the determination of the crack shape is difficult. On the basis of this discussion, several inversion schemes were examined. Finally, a new inversion scheme was found to be successful in estimating the accurate crack size.

(3) Numerical simulations were carried out to investigate the usefulness of the proposed method. The results showed that crack location and shape and loading stress were determined efficiently with good accuracy. CPU time needed to solve the problem was very short, about one minute using the workstation SUN ELC 4/25 FM-8. The proposed method was useful even for the deep crack in the range that  $b/a \leq 2.0$  and  $a/bx \geq 1/100$  in Fig. 1.

### Appendix

Consider an embedded circular crack whose radius  $a$  in an infinite body subjected to uniform tension  $\sigma^\infty$  at infinity, as illustrated in Fig. A-1. By means of the body force method, the crack is replaced by the distribution of body force doublets in an infinite body without a crack. The

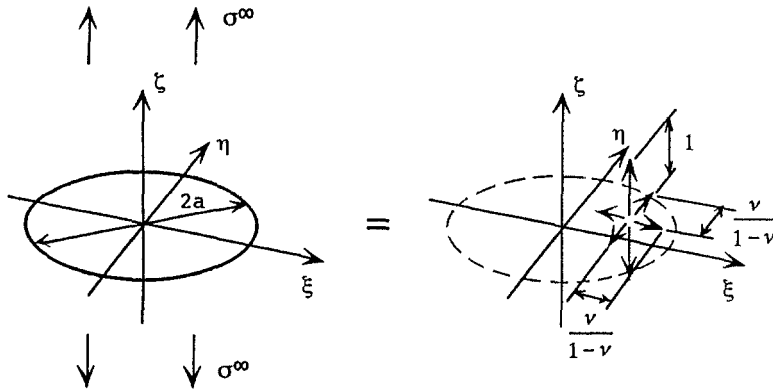


Fig. 16. Fig. A-1 Circular crack in an infinite body.

exact density of the body force doublet distributed on the imaginary crack surface has been given in the following closed form

$$w(\xi, \eta) = \frac{8(1-\nu)^2 a \sigma^\infty}{(1-2\nu)\pi} \sqrt{1 - \frac{\xi^2}{a^2} - \frac{\eta^2}{a^2}}, \quad (\text{A-1})$$

where  $\nu$  is Poisson's ratio. The density  $w(\xi, \eta)$  is related with the crack opening displacement  $U_z(\xi, \eta)$  by the following relation

$$w(\xi, \eta) = \frac{E(1-\nu)}{(1-2\nu)(1+\nu)} U_z(\xi, \eta), \quad (\text{A-2})$$

where  $E$  is Young's modulus.

On this idea of the body force method, the circular crack is approximated by the single giant force doublet as shown in Fig. 5. Then, the magnitude  $T$  of the single giant force doublet is determined by integrating the density of the body force doublet  $w(\xi, \eta)$  acting over the crack surface, that is

$$T = \frac{8(1-\nu)^2 a \sigma^\infty}{(1-2\nu)\pi} \iint_S \sqrt{1 - \frac{\xi^2}{a^2} - \frac{\eta^2}{a^2}} d\xi d\eta, \quad (\text{A-3})$$

where  $S$  is the area of the imaginary crack. If we put

$$\xi = \rho \cos \theta, \quad \eta = \rho \sin \theta, \quad d\xi d\eta = \rho d\rho d\theta, \quad (\text{A-4})$$

the magnitude  $T$  is given as follows

$$\begin{aligned} T &= \frac{8(1-\nu)^2 \sigma^\infty}{(1-2\nu)\pi} \int_0^{2\pi} \int_0^a \rho \sqrt{a^2 - \rho^2} d\rho d\theta \\ &= \frac{8(1-\nu)^2 \sigma^\infty}{(1-2\nu)\pi} \left[ -\frac{(a^2 - \rho^2)^{3/2}}{3} \right]_0^a \times 2\pi = \frac{16(1-\nu)^2 \sigma^\infty a^3}{3(1-2\nu)}. \end{aligned} \quad (\text{A-5})$$

From (A-5), the initial value of the crack size  $a_0$ , expressed in (8) is estimated.

## References

1. S. Kubo, T. Sakagami and K. Ohij, *Computational Mechanics '88*, Vol. 1, Springer, Berlin (1988) 12.i.1–5.
2. N. Tada, *International Journal of Fracture* 57 (1992) 199–220.
3. F. H. Davis and W. J. Plumbridge, *Fatigue and Fracture of Engineering Materials and Structures* 11(4) (1988) 241–250.
4. M. P. Connolly, D. H. Michael and R. Collins, *Journal of Applied Physics* 64(5) (1988) 2638–2647.
5. H. Okada, W. Zhao, S. N. Atluri and S. G. Sampath, *Engineering Fracture Mechanics* 43(6) (1992) 911–921.
6. M. Saka and Y. Takanaka, *Transactions of the Japan Society of Mechanical Engineers* 56A (1990) 1736–1743.
7. M. Saka, *Key Engineering Materials* 51 (1990) 489–494.
8. M. Tanaka, M. Nakamura and K. Yamagiwa, *Boundary Element Method in Applied Mechanics*, Pergamon Press, Oxford (1988) 435.
9. D. H. Chen and H. Nisitani, *Engineering Fracture Mechanics* 45(5) (1993) 671–685.
10. N. Nishimura and S. Kobayashi, *International Journal for Numerical Methods in Engineering* 32(7) (1991) 1371–1387.
11. M. McIver, *IMA Journal of Applied Mathematics* 47 (1991) 127–145.
12. H. Nisitani, *Mechanics of Fracture 5*, Noordhoff International Publishing, Leyden (1978) 1.
13. H. Nisitani and Y. Murakami, *International Journal of Fracture* 10 (1974) 353–368.
14. Y. Murakami and S. Nemat-Nasser, *Engineering Fracture Mechanics* 17 (1983) 193–210.